

# PHYSICAL REVIEW LETTERS

---

---

VOLUME 83

20 SEPTEMBER 1999

NUMBER 12

---

---

## Measurement of the Density Matrix of a Longitudinally Modulated Atomic Beam

Richard A. Rubenstein, David A. Kokorowski, Al-Amin Dhirani, Tony D. Roberts, Subhadeep Gupta, Jana Lehner, Winthrop W. Smith,\* Edward T. Smith, Herbert J. Bernstein,† and David E. Pritchard

*Massachusetts Institute of Technology, Cambridge, Massachusetts 02139*

(Received 26 March 1999)

We present the first measurement of the longitudinal density matrix of a matter-wave beam. Using a unique interferometric scheme, both the amplitude and phase of off-diagonal density matrix elements were determined directly, without the use of traditional tomographic techniques. The measured density matrix of a doubly amplitude modulated atomic sodium beam compares well with theoretical predictions.

PACS numbers: 03.75.Be, 03.75.Dg, 39.20.+q

The determination of the density matrix, or equivalently the Wigner function, of an ensemble of identically prepared particles has long been a subject of interest in quantum measurement theory [1–3] because such distributions contain the most complete description of the quantum state of the system. Recent experiments in this rapidly advancing field have measured the density matrix and/or Wigner function of photon states [4], the vibrational mode of a diatomic molecule [5], and trapped ions [6]. In the field of atom optics, the Wigner function for the transverse quantum state of atoms passing through a double slit has been measured tomographically [7].

In contrast to quantum state tomography (e.g., based on the inverse Radon transformation), newly proposed interferometric methods for determining a density matrix require fewer measurements and permit more straightforward density matrix reconstruction [8–11]. In this Letter, we realize the first interferometric scheme [8] capable of measuring the phase as well as the amplitude of a longitudinal density matrix. Since we have previously shown [12], using a phase-insensitive technique, that a supersonic beam has no nonzero, off-diagonal elements, we first created a density matrix with off-diagonal structure using two sequential amplitude modulators. We then measured the amplitude and phase of this density matrix, demonstrating excellent agreement with predictions.

Study of the longitudinal density matrix of an atomic beam presents special challenges. Working in the energy

basis with eigenkets  $|\Omega\rangle$  and corresponding energy eigenvalues  $\hbar\Omega$ , the density matrix can be written as

$$\begin{aligned}\rho(\Omega', \Omega' + \Omega_{\text{coh}}, t) &= \overline{\langle \Omega' + \Omega_{\text{coh}} | \psi \rangle \langle \psi | \Omega' \rangle} \\ &= \rho_o(\Omega', \Omega' + \Omega_{\text{coh}}) e^{i\Omega_{\text{coh}}(t-t_o)},\end{aligned}\quad (1)$$

where the overbar represents an ensemble average and  $\rho_o$  is the density matrix at time  $t_o$ . Because the density matrix is *intrinsically* time dependent, with elements oscillating at a higher frequency the further off diagonal, a time-dependent measurement scheme is required. In addition, the nonlinear vacuum dispersion relation

$$\Omega(k) = \hbar k^2 / 2m \quad (2)$$

for matter waves reflects the strong dependence of phase velocity on  $k$ . Consequently, the finite energy spread of available atomic beams leads to dephasing which washes out any upstream amplitude modulation of atomic probability [13,14]. The differentially detuned separated oscillatory field (DSOF) technique overcomes these difficulties by heterodyning high frequency off-diagonal density matrix elements to more easily detectable low frequencies and by imparting a momentum dependent phase shift [8,15,16] that reverses the dephasing associated with matter-wave propagation.

In our experiment (see Fig. 1) an incident Na beam [12,14] was first state selected by a two-wire Stern-Gerlach magnet, which transmitted only the  $|F = 1, m_F = 0\rangle$

state. The beam then encountered the two AM zones, narrow oscillatory magnetic field regions separated by  $L_c = 11.3$  cm which were synchronously driven by an amplitude modulated radio-frequency signal with a modulation frequency  $\omega_m = 2\pi \times 60.9$  kHz (the carrier frequency was  $\omega_c = 2\pi \times 7.65$  MHz). These regions

transferred population from the initial  $|1, 0\rangle$  state to both the  $|1, 1\rangle$  and  $|1, -1\rangle$  states.

Solving the three-state resonance problem for the initial plane wave  $e^{i(k_o x - \Omega_o t)}|1, 0\rangle$  propagating through the two AM regions [17], we find the amplitude modulated  $|1, 0\rangle$  state wave function downstream of the second AM region,

$$|\psi(x, t)\rangle = [\cos(\theta_1 \sin\{\omega_m[x/v - (t - L_c x/v)]\}) \cos\{\theta_2 \sin[\omega_m(x/v - t)]\} - \cos\phi_B \sin(\theta_1 \sin\{\omega_m[x/v - (t - L_c/v)]\}) \sin\{\theta_2 \sin[\omega_m(x/v - t)]\}] e^{i(k_o x - \Omega_o t)} |1, 0\rangle, \quad (3)$$

where  $\theta_i = (\frac{\omega_{Ri} l_i}{v})$ ,  $\omega_{Ri}$  is the Rabi frequency,  $l_i$  is the length of the  $i$ th AM region,  $v$  is the atomic velocity, and

$$\phi_B(z) = \frac{\mu_o}{2\hbar v} \int_0^{L_c} B(x, z) dx - \frac{\omega_c L_c}{v}. \quad (4)$$

The first term on the right-hand side of Eq. (4) denotes the relative phase evolved between the  $|1, 0\rangle$  and the  $|1, 1\rangle$  components in traveling between the AM regions, while the second denotes the phase evolved by the oscillatory field during this interval.

The amplitude modulated wave function of Eq. (3) possesses an infinite ladder of energy/momentum sidebands [14], and leads to an energy basis density matrix of the form of Eq. (1) with nonzero elements (or coherences) only at  $\Omega_{\text{coh}} = 2n\omega_m$  for integer  $n$ . The ensemble average includes an average over all atomic velocities and over all possible trajectories through the two AM regions. Variations in magnetic field  $B$  with the vertical coordinate  $z$  between the two AM regions cause the phase  $\phi_B$  in Eqs. (3) and (4) to vary over more than  $2\pi$ , eliminating the second term on the right-hand side of Eq. (3) in the ensemble average.

To explain our DSOF interferometer [14] deconvolution scheme, we consider an atomic beam with a density matrix of the form of Eq. (1), which contains two plane wave components, both in the  $|1, 0\rangle$  electronic state, but with kinetic energy difference  $\hbar\Omega_{\text{coh}}$  after it emerges

from the second AM region at  $x = 0$  (see Fig. 1). It then propagates through two DSOF regions located at  $x_1$  and  $x_2 = x_1 + L$ , where rf magnetic fields of frequencies  $\omega_{1,2}$  drive  $|1, 0\rangle \rightarrow |2, 0\rangle$  hyperfine transitions with resonance frequency  $\omega_{hf} = 2\pi \times 1772$  MHz. The beam then propagates through a state selecting magnet, and the  $|2, 0\rangle$  state is detected at  $x_d$ . This configuration is a longitudinal interferometer, in which the component of state  $|1, 0\rangle$  with kinetic energy  $\hbar\Omega'$  excited to  $|2, 0\rangle$  by  $\omega_1$  and the  $\hbar(\Omega' + \Omega_{\text{coh}})$  component excited by  $\omega_2$  can interfere, producing a time-dependent beat at the detector with frequency  $\delta - \Omega_{\text{coh}}$ , where

$$\delta = \omega_1 - \omega_2. \quad (5)$$

We obtain the density matrix from a measurement of  $P(\delta, \tilde{\delta}, t)$ , the total probability that an atom will reach the detector in the  $|2, 0\rangle$  state after passing through the double AM and the DSOF as a function of  $\delta$  and the ‘‘scaled detuning’’

$$\tilde{\delta} = \frac{\omega_2 x_2 - \omega_1 x_1}{L} - \omega_{hf}. \quad (6)$$

For the case of our fast atomic beam, the double Fourier transform of  $P(\delta, \tilde{\delta}, t)$  with respect to time  $t$  and  $\tilde{\delta}$  determines the complete density matrix [8]

$$\rho_o(\Omega', \Omega' + \Omega_{\text{coh}}) = A(\Omega') \int d\tilde{\delta} e^{-i\tilde{\delta}\sqrt{mL^2/2\hbar\Omega'}} \times \int dt P(\delta, \tilde{\delta}, t) e^{-i(\delta - \Omega_{\text{coh}})t}, \quad (7)$$

where  $A(\Omega')$  is defined in Ref. [8].

The extremely large kinetic energy of our beam relative to the energy shifts applied in the AM regions and the DSOF ( $\Omega_o \gg \omega_m, \delta$ ) permits the use of a semiclassical approximation to obtain a physically intuitive picture of our deconvolution scheme. In this limit, the near field approximation [13] to the quantum wave equation leads to solutions in which the atom's external motion follows raylike classical trajectories, while its internal state evolves quantum mechanically. Thus, the detection probability  $P(\delta, \tilde{\delta}, t)$  is the ensemble averaged product of the double AM transmission probability  $P_{\text{AM}}$  [absolute value squared

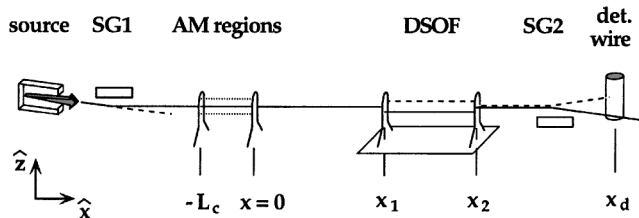


FIG. 1. Apparatus schematic. The atomic beam is state selected by Stern-Gerlach magnet SG1. The resulting  $|1, 0\rangle$  state beam (solid line) travels through AM regions at  $x = -L_c$  and  $x = 0$ , which drive transitions to the undetected  $|1, 1\rangle$  and  $|1, -1\rangle$  states (dotted lines). Oscillatory field regions at  $x_{1,2}$  with frequencies  $\omega_{1,2}$  drive hyperfine state changing transitions, forming the DSOF interferometer. The  $|2, 0\rangle$  state (dashed line) is selected by a second Stern-Gerlach magnet SG2 and detected using a Re hot wire.

of Eq. (3) averaged over  $\phi_B$  and the DSOF transmission probability  $P_{\text{DSOF}}$  (calculated in Ref. [13]):

$$P(\delta, \tilde{\delta}, t) = \langle P_{\text{AM}} \times P_{\text{DSOF}} \rangle \\ = \left\langle \left\{ \sum_{n=-\infty}^{\infty} [C_n(\theta_1, \theta_2, \Omega') e^{i[2n\omega_m(t-T)}] \right\} \right. \\ \left. \times \frac{1}{2} \left[ 1 + \cos\left(\frac{\tilde{\delta}L}{v} + \frac{\delta x_d}{v} - \delta t\right) \right] \right\rangle. \quad (8)$$

The  $\langle \rangle$  denotes an average over the initial energy distribution of the atomic beam (approximately Gaussian in velocity space with a mean of 1100 m/s and an rms width of 25 m/s).  $T = x_d/v$  is the transit time of an atom from the second AM coil to the detector. The coefficients  $C_n$  arise from Bessel function expansions [18] of the sine and cosine terms in Eq. (3).

To study an off-diagonal stripe of the density matrix with  $\Omega_{\text{coh}} = 2N\omega_m$  [or equivalently a particular  $n = N$  component of  $P_{\text{AM}}(t)$ ], we set  $\delta = 2N\omega_m$ , heterodyning its time dependence down to dc. A sweep of the scaled detuning  $\tilde{\delta}$  (with  $\delta$  fixed) produces rephased Ramsey fringes [14], whose Fourier transform with respect to  $\tilde{\delta}$  yields the desired stripe of the density matrix. In the semiclassical picture, the amplitude of this stripe is the velocity distribution of the atoms in the beam with  $e^{i(2N\omega_m t)}$  time dependence, while the phase reveals whether atoms at a given velocity arrived in or out of phase with the ‘‘clock’’ set by the heterodyne signal  $\cos(\delta t)$ .

We first probed the diagonal of the double AM density matrix by setting  $\delta = 0$ , making the DSOF equivalent to a standard separated oscillatory field experiment [19]. This configuration yields Ramsey fringes (Fig. 2) centered at the hyperfine resonance  $\omega_1 = \omega_{\text{hf}}$ . The Fourier transform of these fringes with respect to  $\tilde{\delta}$  gives the energy distribution of the atomic beam as modified by the modulation, i.e., the diagonal of the density matrix (Fig. 3a).

To obtain the off-diagonal elements of the density matrix, we had to scan  $\omega_1$  and hence  $\tilde{\delta}$ , while maintaining phase coherence between the two DSOF coils. We

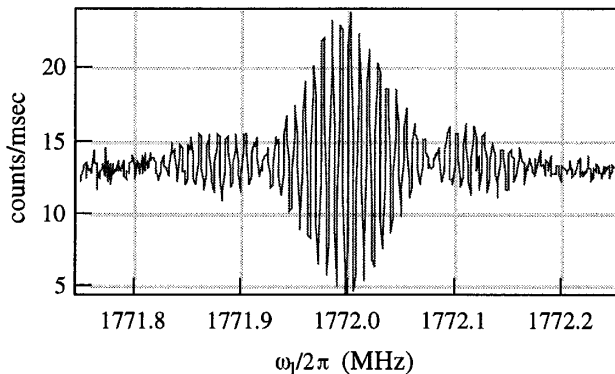


FIG. 2. Ramsey fringes obtained by DSOF with  $\delta = 0$ . The envelope of the fringes reflects the longitudinal atomic energy distribution produced by the AM regions.

achieved this by using a single sideband modulator [20] to generate from  $\omega_1$  a phase coherent signal at  $\omega_2 = \omega_1 - \delta$ . We set  $\delta = 2N\omega_m$  (for  $N = 1, 2$ , and 3) and observed rephased Ramsey fringes which were displaced by  $\frac{\delta(x_d - x_2)}{L} \sim 2\pi N \times 0.6$  MHz from  $\omega_{\text{hf}}$ , where the white fringe condition  $\tilde{\delta}L + \delta x_d = 0$  is satisfied at the detector [see Eq. (8)]. A Fourier transform of the fringes for a particular  $N$  determined a stripe of the density matrix located  $\Omega_{\text{coh}} = 2N\omega_m$  away from the diagonal (as well as its complex conjugate at  $\Omega_{\text{coh}} = -2N\omega_m$ ). At large detunings the DSOF regions produce less than the ideal  $\pi/2$  pulses assumed in Eq. (8), somewhat reducing the signal/noise. This prevented us from measuring the weak off-diagonal stripes for  $N > 3$ .

The amplitude of the density matrix, calculated from an average of two data sets [a total of about 2 h of data with a mean count rate of  $(8-10) \times 10^3$  counts/sec] is shown in Fig. 3a. The multiple peaks along  $\Omega'$  (parallel to the diagonal) for a particular  $n = N$  stripe arise from

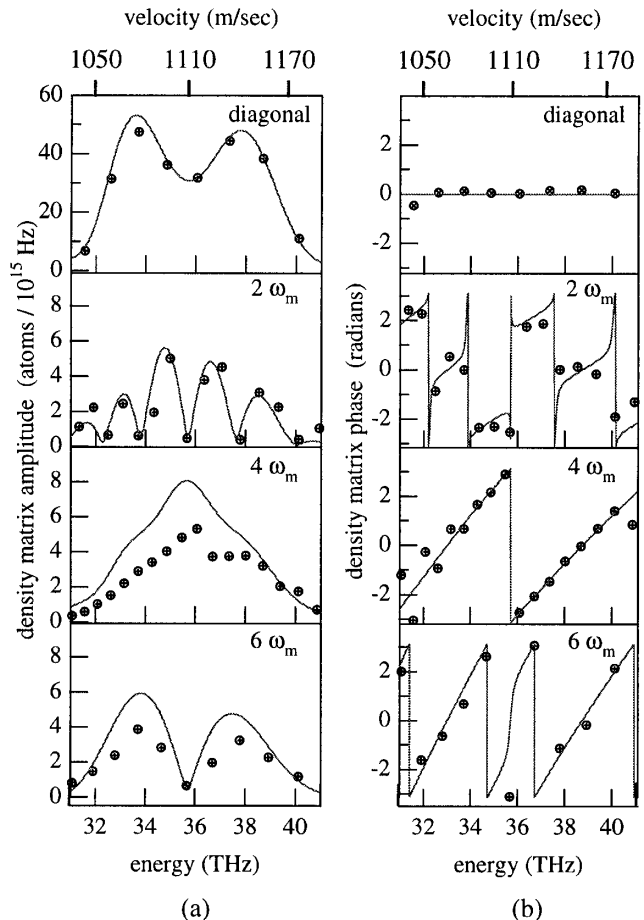


FIG. 3. Measured amplitude (a) and phase (b) of the double AM density matrix with  $\omega_m = 2\pi \times 60.9$  kHz. The solid lines represent the theoretical prediction. The amplitudes are normalized to one for the unmodulated atomic beam. Overall phase offsets have been subtracted from the phase data to compensate for the random phase between sidebands.

the interference of plane wave components that accrue relative phase shifts (by multiples of  $2\omega_m L_c/v$ ) while propagating from the first to the second AM region. In the semiclassical picture, these peaks reflect the velocity selection of the two AM regions, which together transmit only atoms whose transit times  $\tau = L_c/v$  are near multiples of the modulation period  $T_{\text{mod}} = 2\pi/(2N\omega_m)$ .

The phase of the density matrix is displayed in Fig. 3b. The positive and negative phase regions correspond to velocities in and out of phase with the DSOF heterodyne signal. The overall slopes of the phases reflect the velocity dependence of the transit time between the AM coils,  $L_c/v$ . The relative phase between different  $\Omega_{\text{coh}}$  stripes could not be directly determined because the phase of our single sideband mixer was randomized each time the heterodyne frequency  $\delta$  was changed.

A theoretical prediction for the density matrix was obtained by calculating the  $C_n$  of Eq. (8) corresponding to each stripe (i.e., for each  $2n\omega_m$  term) and multiplying it by the initial energy distribution (obtained from an SOF scan of the unmodified beam). By comparing the measured phase of each density matrix stripe with that of our prediction, we determined the phase offset of each stripe, which we subtracted to obtain the comparison displayed in Fig. 3b.

The excellent fits obtained required slight variations of the Rabi frequencies  $\omega_{R1}$  and  $\omega_{R2}$  and the velocity distribution of the beam. These variations were always within the error of independent measurements of these quantities:  $\sim 0.2\%$  for the mean velocity,  $\sim 4\%$  for the velocity width, and  $\sim 10\%$  for  $\omega_{R1}$  and  $\omega_{R2}$ . The large error in  $\omega_{R1,2}$  reflects the hysteresis in the AM driver circuit [20].

We have employed a longitudinal DSOF interferometer [14] to measure the density matrix of a doubly amplitude modulated atomic beam in the longitudinal energy/momentum basis. We found that this density matrix possesses the complex structure predicted theoretically both along and off the diagonal. This work is the first experimental demonstration of such a measurement (the subject of several theoretical proposals [8,15,16]), and it extends previous measurements of the density matrix and Wigner function [4–7] to longitudinally coherent matter waves.

Future experimental realizations could improve the phase control of the single sideband mixer which would then allow direct determination of the relative phase between off-diagonal stripes of the density matrix. The extension of this work to cold atom or Bose-Einstein condensate beams [21,22], which possess low energies and narrow energy widths, would allow the study of density matrices of these highly coherent quantum systems.

We thank R. Lutwak, K. Helmerson, and W. Phillips of NIST and D. Fried, T. Killian, and D. Kleppner of

MIT for the loan of frequency synthesizers. This work was supported by Army Research Office Contracts No. DAAH04-94-G-0170, No. DAAH04-95-1-0533, No. DAAG55-97-1-0236, and No. DAAG55-98-1-0429, Office of Naval Research Contract No. N000014-96-1-0432, Joint Services Electronics Program Contracts No. DAAH04-95-1-0038 and No. DAAG55-98-1-0080, and National Science Foundation Grant No. PHY-9514795. J. L. was supported by the Max Planck Society, and H. B. acknowledges the support of National Science Foundation Grant No. PHY-9722614.

\*Present address: Physics Department, University of Connecticut U-46, 2152 Hillside Road, Storrs, CT 06269.

†Present address: Hampshire College and Institute for Science and Interdisciplinary Studies, Amherst, Massachusetts 01002.

- [1] W. Pauli, *General Principles of Quantum Mechanics* (Springer, Berlin, 1980).
- [2] U. Fano, *Rev. Mod. Phys.* **29**, 74 (1947).
- [3] Special issue on *Quantum State Preparation and Measurement* [*J. Mod. Opt.* **44** (1997)].
- [4] D. T. Smithey, M. Beck, M. G. Raymer, and A. Faridani, *Phys. Rev. Lett.* **70**, 1244 (1993).
- [5] T. J. Dunn, I. A. Walmsley, and S. Mukamel, *Phys. Rev. Lett.* **74**, 884 (1995).
- [6] D. Leibfried *et al.*, *Phys. Rev. Lett.* **77**, 4281 (1996).
- [7] Ch. Kurtsiefer, T. Pfau, and J. Mlynek, *Nature (London)* **386**, 150 (1997).
- [8] A. Dhirani *et al.*, *J. Mod. Opt.* **44**, 2583 (1997).
- [9] M. Freyberger, S. H. Kienle, and V. P. Yakovlev, *Phys. Rev. A* **56**, 195 (1997).
- [10] S. H. Kienle *et al.*, *Appl. Phys. B* **65**, 735 (1997).
- [11] I. A. Walmsley and N. P. Bigelow, *Phys. Rev. A* **57**, R713 (1998).
- [12] R. A. Rubenstein *et al.*, *Phys. Rev. Lett.* **82**, 2018 (1999).
- [13] D. E. Pritchard *et al.*, *Phys. Rev. A* **59**, 4641 (1999).
- [14] E. T. Smith *et al.*, *Phys. Rev. Lett.* **81**, 1996 (1998).
- [15] D. Kokorowski and D. Pritchard, *J. Mod. Opt.* **44**, 2575 (1997).
- [16] M. Raymer, *J. Mod. Opt.* **44**, 2565 (1997).
- [17] The applied transverse guide field ( $\sim 10$  G) was small enough to neglect the quadratic term in Zeeman energy, so the  $|1, 0\rangle \rightarrow |1, 1\rangle$  and  $|1, 0\rangle \rightarrow |1, -1\rangle$  transitions had approximately equal resonance frequencies.
- [18] G. Arfken, *Mathematical Methods for Physicists* (Academic Press, San Diego, 1985), pp. 576–578.
- [19] N. F. Ramsey, *Molecular Beams* (Oxford University Press, Oxford, 1956).
- [20] R. A. Rubenstein, Ph. D. thesis, Massachusetts Institute of Technology, 1999.
- [21] M.-O. Mewes *et al.*, *Phys. Rev. Lett.* **78**, 582 (1997).
- [22] M. R. Andrews *et al.*, *Science* **275**, 637 (1997).